scientific reports

Check for updates

OPEN

Novel fully human IgG1 targeting folate receptor α demonstrates antitumor efficacy driven by avidity rather than monovalent binding affinity

Elena Pinto[1,8], Davide Tresoldi[1,8], Valeria Arlotta[1], Elena Luison[1], Barbara Frigerio[1], Elisa Corsiero[1,2], Francesco Raspagliesi[3], Sophia N. Karagiannis[4,5], Silvana Canevari[6], Delia Mezzanzanica[7,9] & Mariangela Figini[1,9]✉

Folate receptor alpha (FRα), a membrane protein involved in folate transport, is a promising therapeutic target for ovarian cancer and other malignancies. The murine Monoclonal antibody (MAb) MOv19, developed in our lab, has pioneered the development of chimeric antibody-drug conjugates currently approved or in clinical trials for the treatment of FRα-positive cancers. To further reduce antibody's immunogenicity, we engineered and characterized a new fully human IgG1 antibody (AFRA hIgG1) to FRα starting from MOv19. AFRA hIgG1 was constructed and characterized for binding affinity, specificity to purified FRα and various FRα-expressing tumor cells and ability to recruit effector cells in vitro in comparison to the chimeric version of MOv19 (ChiMOv19). AFRA hIgG1 and ChiMOv19 have comparable functional affinities being 10^{-9} M and 10^{-10} M, respectively although AFRA hIgG1 has an intrinsic constant affinity 10^3 lower than that of ChiMOv19, 2.6×10^{-7} M vs. 3.5×10^{-10} M, respectively. Furthermore, AFRA hIgG1 demonstrated a better binding kinetic with an overall efficacy comparable to ChiMOv19 in recruiting effector cell functions. These findings highlight that functional affinity, rather than intrinsic affinity, is a key determinant of biological response. AFRA hIgG1 shows promise as a biologic agent for the treatment of FRα-positive cancers.

Keywords Human monoclonal antibody, Antibody engineering, Targeted therapy, PBMCs-mediated cytotoxicity, Intrinsic affinity, Functional affinity

Abbreviations

ATCC	American Type Culture Collection
BSA	Bovine Serum Albumin
ELISA	Enzyme-linked immunosorbent assay
FACS	Fluorescence-activated cell sorting
Fab	Fragment antigen-binding
F(ab)2	Divalent antibody fragment
FRα	Folate receptor alpha
HBS-EP+	Hepes-bufferred saline with surfactant 20

[1]ANP 2 Unit, Fondazione IRCCS Istituto Nazionale dei Tumori, 20133 Milan, Italy. [2]Centre for Experimental Medicine and Rheumatology, William Harvey Research Institute, Barts and The London School of Medicine and Dentistry, Queen Mary University of London, London EC1M 6BQ, UK. [3]Gynecologic Oncologic Unit, Fondazione IRCCS Istituto Nazionale dei Tumori, 20133 Milan, Italy. [4]St. John's Institute of Dermatology, School of Basic and Medical Biosciences and KHP Centre for Translational Medicine, King's College London, Guy's Hospital, London, UK. [5]Breast Cancer Now Research Unit, School of Cancer and Pharmaceutical Sciences, King's College London, Guy's Cancer Centre, London, UK. [6]Segrate, Italy. [7]Integrated Biology of Rare Tumors Unit, Dept. of Experimental Oncology, Fondazione IRCCS Istituto Nazionale dei Tumori, 20133 Milan, Italy. [8]Elena Pinto and Davide Tresoldi contributed equally to this work. [9]Delia Mezzanzanica and Mariangela Figini contributed equally to this work. ✉email: mariangela.figini@istitutotumori.mi.it

HRP	Horseradish peroxidase
IgG	Immunoglobulin G
Mab	Monoclonal Antibody
MCK	Multi-cycle kinetics
PBMC	Peripheral blood mononuclear cells
PBS	Phosphate-buffered saline
PIPE	Polymerase Incomplete Primer Extension
POCC	Primary ovarian cell cancer line
SDS-PAGE	Sodium dodecyl sulfate-polyacrylamide gel electrophoresis
SEC	Size exclusion chromatography
SCK	Single-cycle kinetics
VH	Heavy-chain variable
VL	Light-chain variable

Folate receptor alpha (FRα) is a 38 kDa glycosylphosphatidylinositol (GPI) - anchored membrane protein involved in folate binding and transport[1]. The expression of FRα in normal tissues is restricted to a few compartments (i.e., uterus, placenta, choroid plexus, lung, and kidney), where it localizes to the apical and luminal surface of polarized epithelial cells, precluding its contact with the circulation[2–4]. Conversely, in the context of malignancy, FRα is overexpressed on the entire cell surface, thus losing its polarized cellular localization. The different localization of the FRα within normal tissue and in tumours makes this receptor a promising candidate for targeted therapy[5–7]. FRα is overexpressed in a wide range of solid malignancies such as mesothelioma, ovarian, lung, breast (including the triple negative subtype) cancer and head and neck tumours[8–11]. Very importantly, FRα expression is not altered by chemotherapy supporting the rationale for FRα–targeted therapies both at tumour diagnosis and at recurrence[12,13].

MOv19 was one of the first murine MAb generated against FRα and was obtained in our laboratory[14] thus providing the basis for the generation of several MOv19 variants using antibody engineering strategies[15]. Currently, two MOv19 derivatives have entered into clinical trials: (i) a chimeric resurfaced version in an antibody-drug conjugate format, Mirvetuximab-Soravtansine[16,17], is the first ADC anti-FRα approved by FDA[18] and (ii) the murine scFv in a second-generation chimeric T cell antigen receptor, CAR-T (Phase Ia)[19]. Considering the favourable clinical impact of these MOv19 derivatives, to develop a less immunogenic therapeutic MAb, we initially constructed a fully human anti-FRα Fab fragment (VHCH1 + VLCL) by using combinatorial phage display libraries, derived from healthy donors or from ovarian cancer patients. To obtain a competing antibody recognising the same or an overlapping epitope, we used the epitope imprinting selection method, known as guided selection[20,21] to avoid chanche of recongnizing different epitopes that may results in different behaviors. The light chain of murine MOv19 was used to drive the selection of human Ab chains against FRα[22]. One of the selected human fragments (AFRA5.3), after optimization as a chemical dimer (AFRA5.3-DFM), undergone evaluation for radioimmunotherapy in ovarian cancer[23].

Considering its performance, in this study we used the variable domains of AFRA5.3 human Fab fragment, for the construction of a new fully human IgG anti-FRα MAb (AFRA hIgG1) to study its ability in recruiting cytotoxic effector cells. AFRA hIgG1 binding affinity and specificity were analyzed towards the purified FRα protein and several FRα-expressing tumour cells in comparison to the chimeric version of the murine MOv19 (ChiMOv19), in which the original antibody murine constant CL and CH γ2a chains were replaced by human constant CL and CH γ1 domains[24]. Finally, AFRA hIgG1 and ChiMOv19 were compared and characterized for their ability to recruit effector cells in vitro.

The successful development and characterization of AFRA hIgG1 could pave the way for more effective treatment options for patients with FRα-expressing cancers, potentially overcoming current challenges in drug efficacy and safety.

Results

AFRA hIgG1 construction and characterization

The fully human AFRA-hIgG1 antibody was obtained after cloning the variable VH and VL sequences of AFRA5.3 into the pVITRO hIgG1K vector allowing the assembling of a intact human IgG. (See Supplementary Fig. S1). The vector was then transfected into the FreeStyle™ 293 cells grown in appropriated Higromycin B selection medium for isolation of cells producing AFRA hIgG1 that was then purified from cell culture supernatant with a yield of up to 10 mg/L.

Purified AFRA hIgG1 and ChiMOv19 consisted mainly of monomeric molecules (150 kDa) with a marginal amount (less than 4%) of aggregates and dimers, assessed by Coomassie stained SDS–PAGE (Supplementary Fig. S2a) or evaluated by Size Exclusion Chromatography (SEC) (Supplementary Fig. S2b, c).

Relevance for isoelectric points (pI) charateristics is mainly due to the antibodies' constant domain. In fact, as expected, AFRA hIgG1 and ChiMOv19, having the same human constant region, showed a similar pI, although their variable regions (human and murine, respectively) showed different pI (Supplementary Table S3).

ChiMOv19 was used as term of comparison for the new fully human MAb AFRA hIgG1 functional characterizations. Indeed, AFRA hIgG1 antigen recognition derived from the variable chains of AFRA5.3, obtained by epitope imprinting selection guided by the light chain of the murine MOv19[22]. On the other hand, AFRA hIgG1 effector function, mediated by constant chains, derived from the human IgG1 constant chains the same isotype used for the production of the ChiMOv19[24].

To assess the antibody's functional affinity, reflecting bivalent binding of both ChiMOv19 and AFRA hIgG1, a Biacore single cycle kinetics (SCK) technique, allowing determination of binding kinetics in a single injection cycle, was applyied by sequential injections of different concentrations of analyte over a surface with immobilized

ligand. This method is particularly useful when regeneration of the surface between binding cycles is difficult or detrimental to the ligand.

Using a 1:1 interaction method AFRAhIgG1 exhibited a KD of 1.2×10^{-9} M, while ChiMOv19 showed a KD of 2.6×10^{-10} M (Fig. 1a,b). The values of the kinetic of binding calculated using the bivalent method are available in the Supplementary Table S1.

The antibodies' monovalent binding, defined as intrinsic affinity, was measured using the classical multi cycle kinetics (MCK) by immobilizing the antibody on the sensor chip and using the FRα as analyte to ensure a 1:1 interaction. The association rates for AFRA hIgG1 is 1.3 time faster than that of ChiMOv19 whereas the dissociation rate is exremely faster (Kd = 0.27 1/s) compared to that of ChiMOv19 (Kd = 4.5×10^{-4} 1/s) (Fig. 1c,d). As the affinity constant (KD) is calculated as a ratio of Kd/Ka, this implies that the affinity constant was much lower for AFRA hIgG1 (2.6×10^{-7} M) in comparison to ChiMOv19 (3.5×10^{-10} M), assuming a 1:1 interaction.

Although the intrinsic affinity of AFRA-hIgG1 was substantially lower than that of ChiMOv19, this difference was reduced under functional (bivalent) conditions. Interestingly, AFRA-hIgG1 showed a clear improvement in binding strength in the bivalent context (Fig. 1a compared to Fig. 1c).

To confirm the reproducibility of the binding data, Biacore analyses were performed on two independent production batches of the antibody. The experiments were conducted using the antibody both as the analyte and as the immobilized ligand, ensuring consistency across formats and production lots.

We then assessed the ability of AFRA hIgG1 to retain its specificity for FRα positive tumour cells of different histotype compared to ChiMOv19. AFRA hIgG1 binding specificity was tested by flow cytometry on a large panel

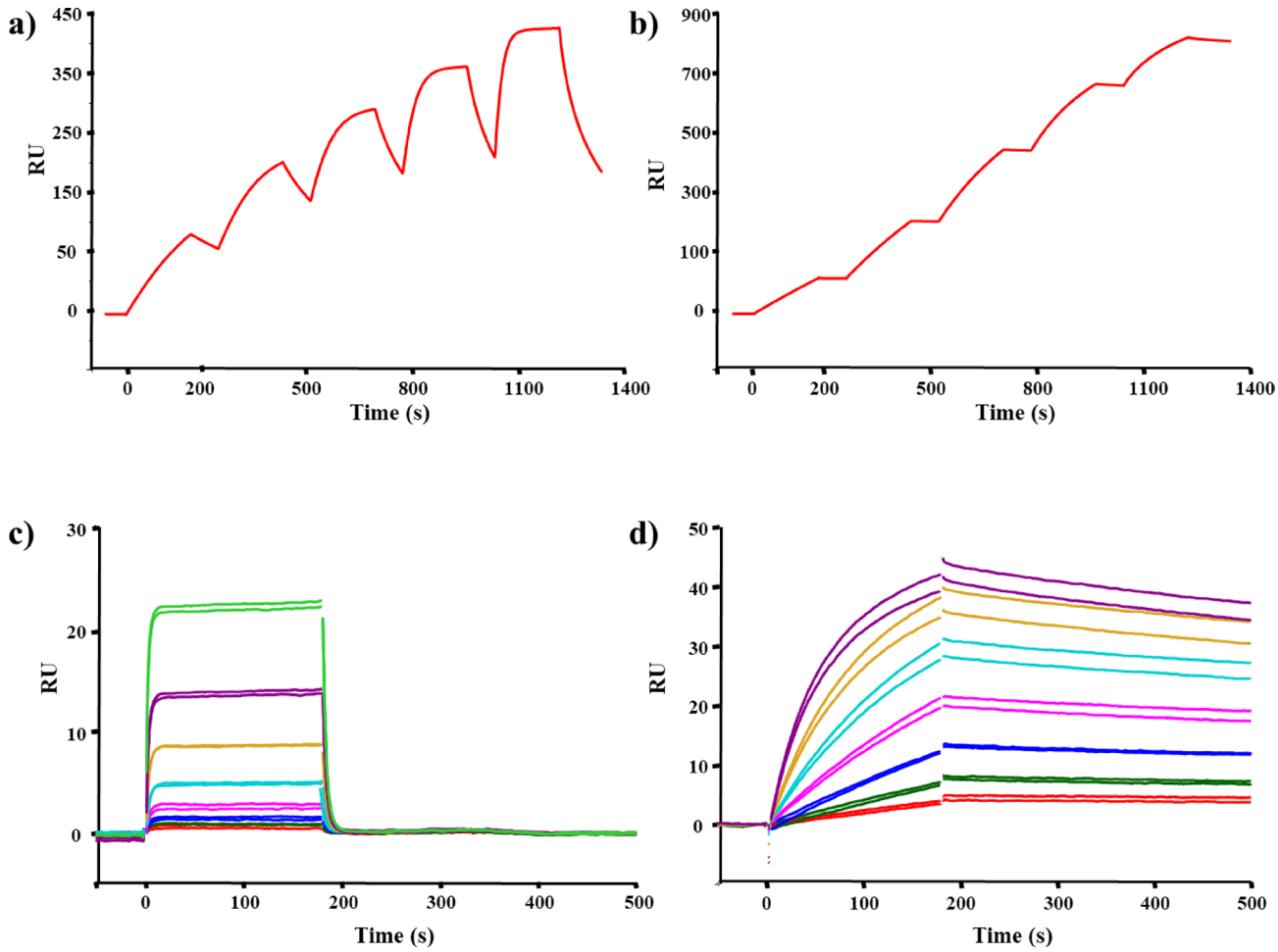

Fig. 1. Affinity measured by SPR analysis of AFRA hIgG1 and ChiMOv19. (**a**, **b**) Functional affinity (measured by SCK). 700 RU of recombinant FRα was immobilized on a CM5 sensor chip. Antibodies were injected in SCK (no regeneration between injections). AFRA hIgG1 and ChiMOv19 were tested from 12.5 to 0.8 nM (**b**). (**a**) AFRA hIgG1: Ka = 6.6×10^{6} (1/Ms), Kd = 0.008 (1/s), KD = 1.2×10^{-9} M, RUmax = 488, χ^2 = 36. (**b**) ChiMOv19: Ka = 9.5×10^{5} (1/Ms), Kd = 2.4×10^{-4} (1/s), KD = 2.6×10^{-10} M, RUmax = 882, χ^2 = 48. (**c**, **d**) Intrinsic affinity (measured by MCK). Soluble recombinant FRα (200–0.4 nM) was injected over immobilized AFRA hIgG1 (**c**) or ChiMOv19 (**d**). (**c**) AFRA hIgG1: Ka = 1.0×10^{6} (1/Ms), Kd = 0.27 (1/s), KD = 2.6×10^{-7} M, RUmax = 67, χ^2 = 0.03. (**d**) ChiMOv19: Ka = 1.3×10^{6} (1/Ms), Kd = 4.5×10^{-4} (1/s), KD = 3.5×10^{-10} M, RUmax = 42, χ^2 = 1.6. Binding is expressed as responsive unit (RU; y-axis) over time (x-axis). Kinetics were obtained by global fitting to a 1:1 model using Biacore T200 software.

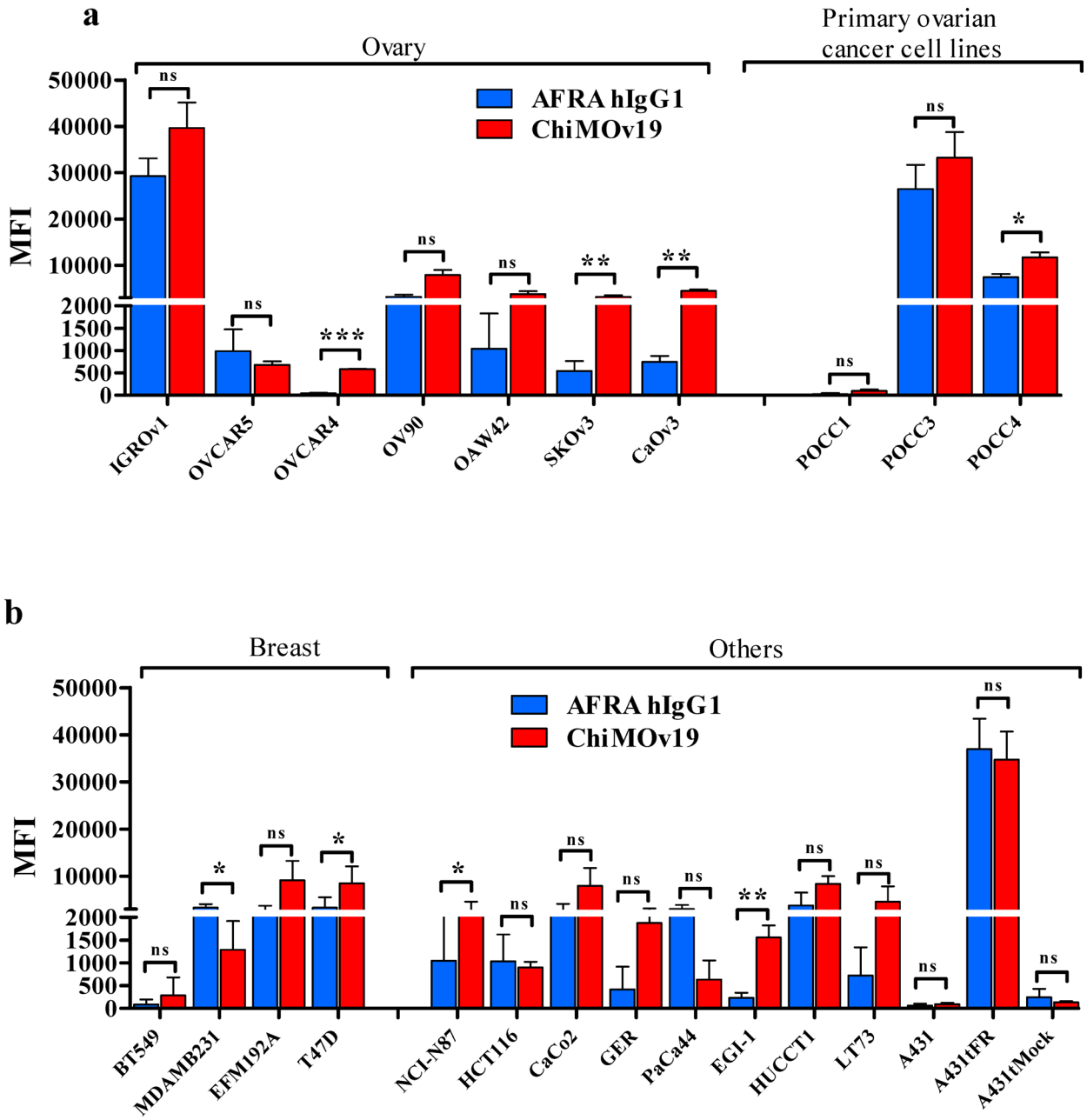

Fig. 2. Flow cytometry analysis of AFRA hIgG1 and ChiMOv19 binding ability and specificity. (**a**) Histograms of mean fluorescence intensities (MFI) of ovarian cancer cell lines and primary cultures of ovary cancer as reported in Supplementary Table S2a. (**b**) Histograms of MFI across multiple cell lines, as reported in Supplementary Table S2b. Two different sizes for y axis scales (bottom $0 < MFI < 2000$ and top $3000 < MFI < 50000$) were used to better appreciate the cell lines that have a low MFI. The red bar corresponds to ChiMOv19; blue bar corresponds to AFRA hIgG1. * $p < 0.05$; ** $p < 0.01$; *** $p < 0.001$; ns: not statistically significant. (**c**) Representative flow cytometry histograms showing AFRA hIgG1 compared to ChiMOv19 binding on highly FRα expressing cell lines (IGROV1 and A431tFR, top left and right, respectively) and FRα negative cells (A431 and A431 tMock, bottom left and right respectively) cell lines. Light blue histograms correspond to AFRA hIgG1 and ChiMOv19 binding; red histograms correspond to a negative control antibody (Alexa 488 anti-human IgG (H + L) antibody).

of cell lines with varying expression levels of FRα and derived from ovarian, breast, digestive tract cancers and mesothelioma (Supplementary Table S2). AFRA hIgG1 and ChiMOv19 specifically bind all the FRα positive cell lines but with different patterns of reactivity. The strongest binding was observed on ovary and breast carcinoma whereas a lower, but still specific, binding was observed on the other cell lines (Fig. 2a, b and Supplementary Table S2). Figure 2c shows representative binding histograms for both MAbs on a highly expressing FRα ovarian

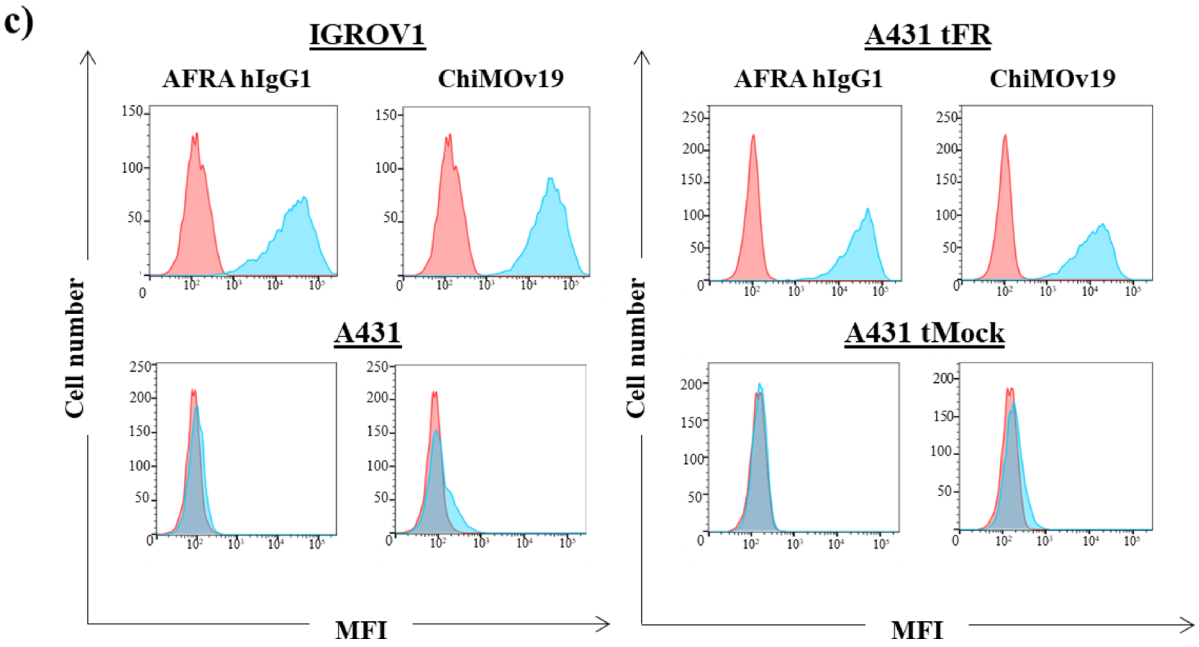

Fig. 2. (continued)

cancer cell line (IGROV1) as well as on a tumor cell line with ectopic expression of FRα (A431tFR) and the corresponding isogenic negative controls (A431 and A431tMock).

Next, we confirmed the binding specificity of AFRA hIgG1 in ELISA using both the FRα positive cell lines, (IGROV1 and A431tFR) and the negative controls, (A431 and A431tMock). As shown in Fig. 3, both antibodies showed a specific and similar binding towards the FRα positive cells and no binding to the negative A431 and A431tMock cells. The pattern of reactivity of the 2 MAbs suggested that they could recognize an overlapping epitope on the same antigen.

Finally, to demonstrate that AFRA hIgG1 and ChiMOv19 recognize the same or overlapping epitopes, we performed competition assay on purified antigen as well as on living cells. As shown in Fig. 4a, AFRA hIgG1 failed to bind to the sensor chip coated with purified FRα that was previously saturated with ChiMOv19, indicating competitive binding for the same or for an overlapping epitope. However, although we cannot completely exclude that quite distal epitopes may also be blocked sterically due to the IgG size compared to the target, a different antibody recognizing a distinct epitope on the FRα (MOv18)[14,24] was still able to bind the antigen on the sensor chip saturated with ChiMOv19.

The same results were observed when the binding competition was performed in living IGROV1 cell line (Fig. 4b), further proving that AFRA hIgG1 and ChiMOv19 recognize an overlapping epitope on FRα. Moreover, the presence of ChiMOv18 did not prevent the binding of AFRA hIgG1 or ChiMOv19; instead, its presence enhanced their binding to FRα, indicating a target's conformational change facilitating the binding of MOv19 derivatives to their epitope, as already shown for the corresponding murine MAbs[25].

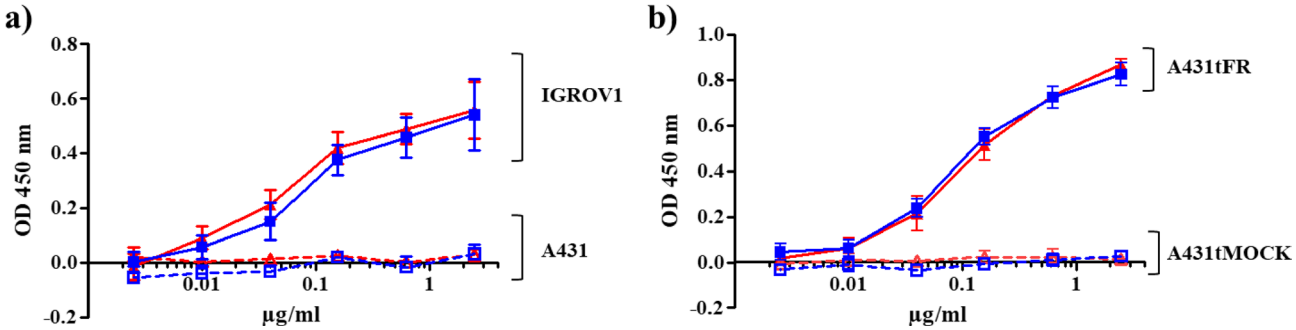

Fig. 3. Binding analysis of AFRA hIgG1 and ChiMOv19 on FRα positive and negative cell lines by ELISA. Graphs reporting the ELISA results showing AFRA hIgG1 (blue line) and ChiMOv19 (red line) binding on (**a**) FRα positive (IGROV1) and negative (A431) cells and (**b**) FRα ectopically expressing cells (A431tFR) and their isogenic negative controls (A431tMock). The results are an average of 5 and 3 experiments respectively.

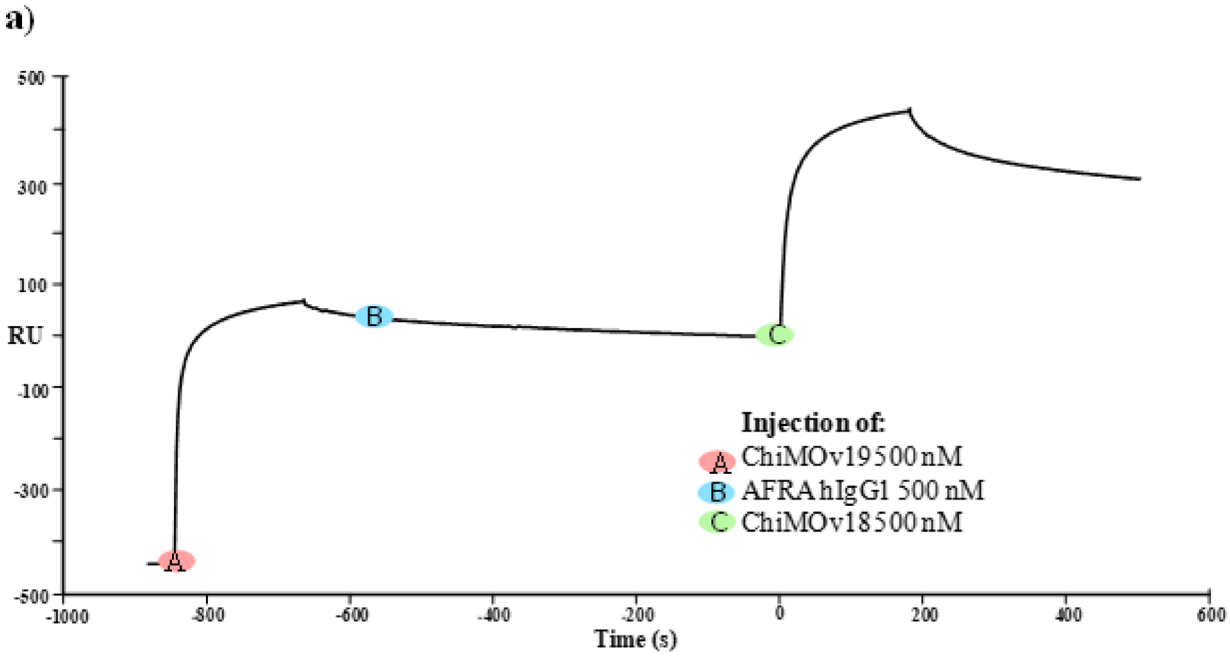

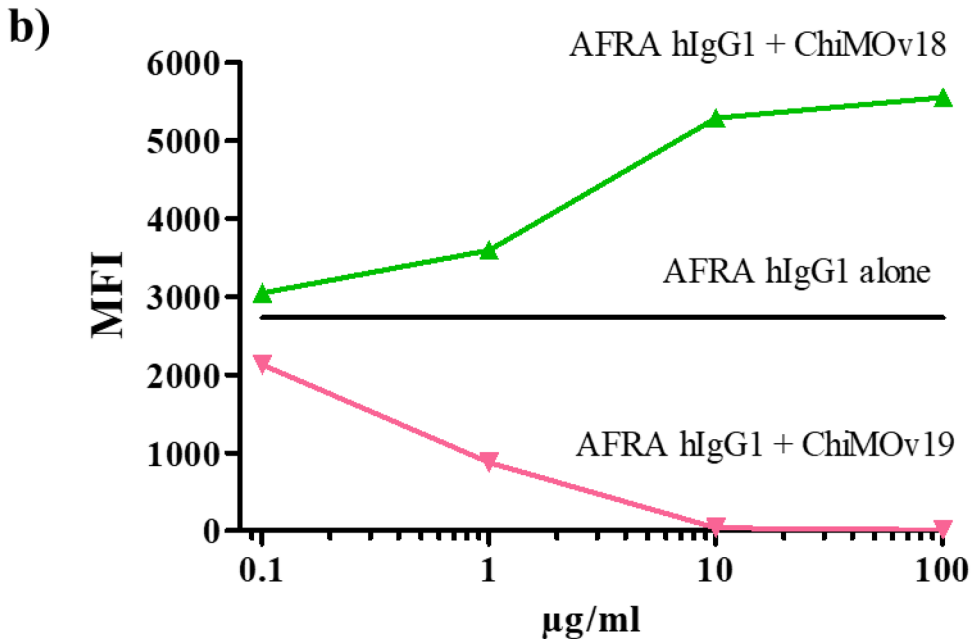

Fig. 4. FRα binding competion. (**a**) Competitive binding studies by SPR on purified FRα. FRα was immobilized on the CM5 sensor chip. ChiMOv19 (500 nM) was first injected of (A), followed by injection of 500 nM of AFRA hIgG1 (B) and of a non-competing anti-αFR antibody ChiMOv18 (C). Binding is expressed as responsive unit (RU; y-axis) over time (x-axis). (**b**) Competition studies by Flow Cytometry on FRα expressing cells (IGROV1). MFI variations (y-axis) in response to increasing concentrations of unlabelled antybody (x-axis). In the graph are rappresented: AFRA hIgG1-Alexa 488 + unlabelled ChiMOv18 (green line), AFRA hIgG1-Alexa 488 + unlabelled ChiMOv19 (pink line) and AFRA hIgG1-Alexa 488 alone (black line).

AFRA hIgG1 stability characterization

AFRA hIgG1 was further analyzed to evaluate its stability after long-term storage, The antibody, stored under sterile conditions in a solution containing 10 mM sodium phosphate (pH 7.4) and 150 mM sodium chloride at 4 °C for up to 6 months, retained its monomeric condition (over 95%) with no increase of aggregate formation

evaluated by SDS-PAGE and SEC analysis (Supplementary Fig. S3a,b) and its functionality as assessed by and ELISA assays (Supplementary Fig. S3c).

Cytotoxicity assay

We then investigated whether AFRA hIgG1 could trigger PBMCs cytotoxicity towards different tumour cell lines. AFRA hIgG1 and ChiMOv19 were initially tested at a concentration of 2 µg/mL on IGROV1 (Fig. 5a) and A431 (Fig. 5b) in presence of PBMCs from healthy donors and cytotoxicity was monitored from 24 to 120 h. The addition of AFRA hIgG1 (blue solid line) to PBMC efficiently inhibited IGROV1 cell growth compared to PBMC alone (solid green line). The inhibition progressed steadily over time from the start of treatment (at 24 h), reaching almost 80% of inhibition at 72 h (Fig. 5) and no inhibition was observed on the FRα negative A431 cells (Fig. 5b). ChiMOv19 shows a similar pattern of inhibition during time (red lines). No inhibition was detected by incubating cells with antibodies alone .

Moreover titration of the antibodies showed that both AFRA hIgG1 and Chi Mov19 specific ADCC activity could be seen at a concentration as low as 0.125 µg/ml (Supplementary Fig. S4).

Considering that the best efficacy was seen at 72 h of incubation, this time point was selected to verfy the ability of AFRA hIgG1 in retargeting the PBMC cytotoxic activity of different healthy donors toward cell lines with different FRα expression levels and of different histotype (Fig. 6).

IGROV1 and A431 were used as positive and negative control, respectively. The best actitivity was observed on cells with the highest FRα expression levels (IGROV1, POCC3 and POCC4) and no activity was recorded on the FRα negative cells (A431 and POCC1). However, on the other cell lines level of cytotoxicity was not proportional to FRα expression, thus suggesting possible mechanisms of intrinsic resistance as we already observed in a context of lymphocyte retargeting triggered by bi-specific antibodies[26]. Moreover, due to the wide variability in observed effects and the limited number of donors, it was not possible to draw definitive conclusions regarding the differences.

Discussion

Folate Receptor Alpha (FRα) is an attractive therapeutic target for an antibody-based treatment since it is highly and widely expressed in many types of cancer while it is absent or expressed only at low levels in most normal tissues[27]. Several anti-FRα monoclonal Abs have been developed including derivatives of the murine MAb MOv19, discovered in our laboratory in the second half of the 1980s[14]. These derivatives were modified and engineered to obtain reagents with reduced immunogenicity that are now either FDA-approved or in clinical trials[18,19].

To further improve efficacy and decrease potential immunogenicity still intrisinc in a chimeric molecule bearing murine residues, we engeneered a fully human MOv19 IgG derivative (AFRA hIgG1), reconstituting the human Fc γ1 portion starting from the MOv19 human Fab fragment (AFRA5.3) obtained by epitope impring selection[22] and we compared its perforamance against the chimeric MOv19 (ChiMOv19).

Considering AFRAhIgG1 binding kinetic, we confirmed our previous work describing the characteristics of the AFRA 5.3 Fab fragment chemically dimerized to obtain a F(ab)2 fragment aimed at exploiting the ability of the radiolabelled antibody to reach the target with suitable functional activity but smaller size compared to a full IgG[22]. Concerning strength of binding, AFRA hIgG1 showed an affinity constant 10^3 lower than that of ChiMOv19 (2.6×10^{-7} M vs. 3.5×10^{-10} M, respectively) consistently with what previously observed[22]. However, this difference was reduced under functional (bivalent) conditions with AFRA-hIgG1 showing a clear improvement in binding strength in the bivalent context with values similar to those of ChiMOv19 (KD of 1.2×10^{-9} M and 2.6×10^{-10} M, respectively) and still in the range of most of the Abs used in the clinic[28]. Since bivalent interactions for an IgG antibody more closely mimic physiological conditions, these results suggest that

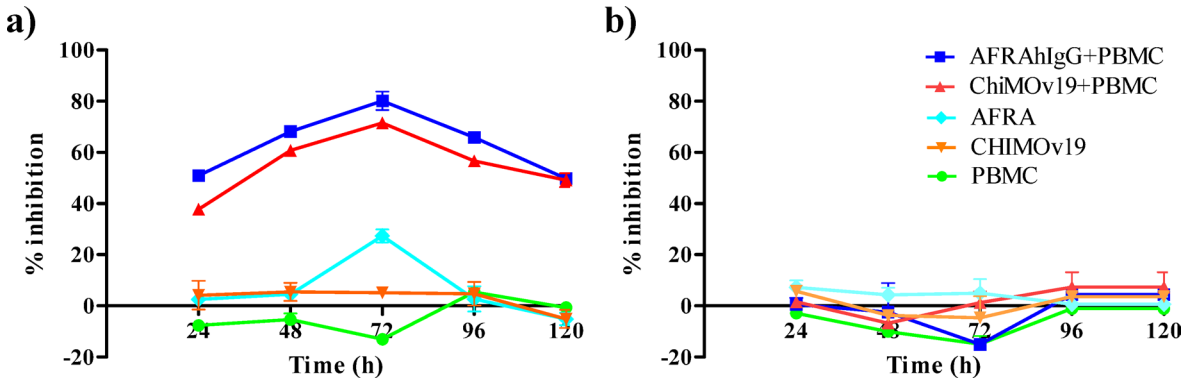

Fig. 5. Antibody-dependent cytotoxicity. Percentage of cell growth inhibition is reported in the presence of: PBMCs alone (green lines), AFRA hIgG1 alone (light blue lines), ChiMOv19 alone (orange lines) or AFRA hIgG1 (blue lines) and ChiMOv19 (red lines) with the addition of PBMC at E: T ratio of 10:1 from 24 to 120 h on FRα positive (IGROV1; Panel **a**) and FRα negative (A431; Panel **b**) cell lines. Antibodies' concentration used was 2 µg/ml. Statistical analysis: IGROV1: AFRA hIgG1 + PBMC vs. PBMC $p < 0.0001$; IGROV1: ChiMOv19 + PBMC vs. PBMC $p < 0.0001$.

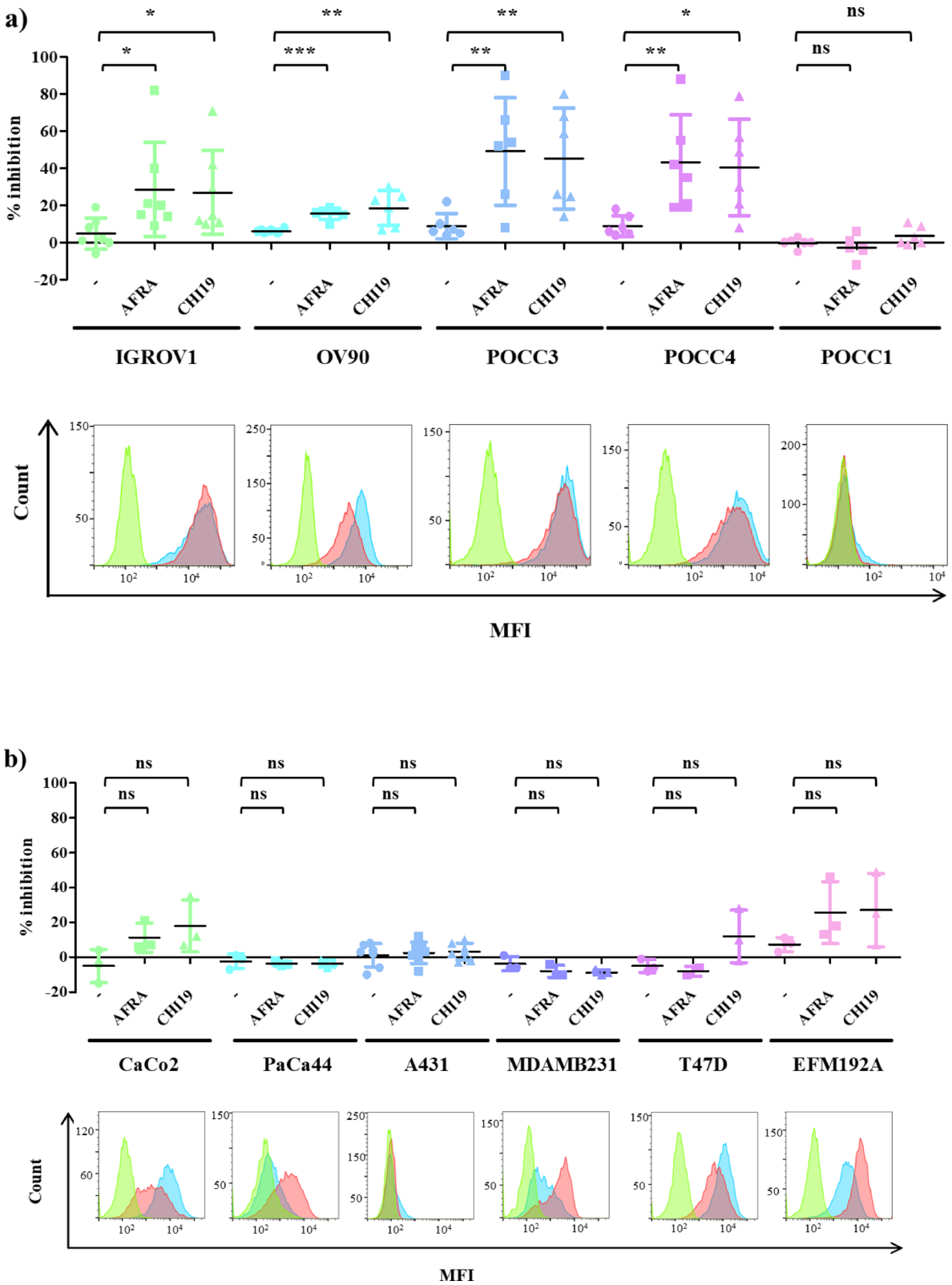

Fig. 6. Antibody-dependent cytotoxicity on cells of different origins. Percentage of cell growth inhibition induced at 72 h by AFRA hIgG1 (squares) or ChiMOv19 (triangles) in the presence of PBMC from different (from 3 to 7) healthy donors compared to PBMCs alone (circles) at E: T ratio of 10:1. Antibodies' concentration used was 2 µg/ml (**a**) ovarian cancer cell lines IGROV1, OV90, and ovarian cancer primary cultures POCC3, POCC4 and POCC1. (**b**) Cell lines from different histotype (see supplementary Table S2 for origin). Flow cytometry panels were added to evaluate FRα expression for each cell line (green histograms: negative control, red histograms: AFRA hIgG1, light blue histograms: ChiMOv19). * $p < 0.05$; ** $p < 0.01$; *** $p < 0.001$; ns: not statistically significant.

functional affinity could be a more relevant indicator of in vivo efficacy than intrinsic (monovalent) affinity. Therefore, optimising an antibody's monovalent affinity may be unnecessary if the final therapeutic format is bivalent. Overall antitumour efficacy correlates far better with *avidity* (the cooperative binding achieved when both antibody's arms engage antigen in vivo) than with monovalent affinity measured in vitro. Hence, future engineering strategies might yield greater clinical benefit by maximising bivalent engagement and functional avidity, rather than by chasing ever-tighter monovalent KD values. Indeed, despite the lower intrinsic affinity, the ability of AFRA hIgG1 to retarget PBMC activity against cancer cells of different origin and expressing different levels of FRα, was comparable to that of ChiMOv19 thus suggesting that functional affinity (considered as avidity and affinity) is the primary determinant of effector recruitment.

Moreover, when the antigen is not overexpressed, as in normal tissues, a quick monovalent binding (Ka) and a fast dissociation (Kd) can be advantageous since it may help in minimizing off-target. effects and reduced toxicity. Indeed, there is scientific evidence that antibodies with lower affinity may be advantageous[29], especially in the context of antibody-drug conjugates (ADCs)[30,31].

Intrinsic binding affinity should be tuned according to antibody's application; in fact, a higher affinity might not be always an advantage. High-affinity IgG that binds internalising receptors may be degraded more rapidly than low-affinity IgG, thus limiting tumour penetration[32]. These so-called "binding site barriers"[33–35] may result in lower quantitative tumour delivery of higher affinity Abs. Indeed, a too-high affinity may result in a high concentration in the perivascular space and a low concentration in the tumour.

All together these data suggest thatthe MAbs' binding affinity does not directly correlate with its function (in this case cytotoxic activity) and that intrinsic tumour-resistance mechanisms to MAb-mediated PBMC citotoxiciy, independent of FRα expression level and to the MAbs' binding affinity, may exist particularly in tumors different than ovarian cancer.

Overall, we described a new fully human MAb, AFRA hIgG1, characterized by a lower binding affinity but a similar binding specificity to FRα compared to the chimeric MAb counterpart. Importantly, thanks to a particular kinetic of binding, despite the lower intrinsic affinity for FRα, AFRA hIgG1 was able to exert similar cytotoxicity in ovarian tumour cells compared to ChiMOv19.

Conclusion

We described a new fully human MAb, AFRA hIgG1, characterized by a lower binding affinity but a similar binding specificity to FRα compared to the ChiMOv19 counterpart. Importantly, our data suggests that the kinetics of binding—particularly the on-rate and off-rate—may play a more critical role in functional activity rather then than their intrinsic affinity.

Materials and methods

Cell lines

Details of the tumour cell lines used in this study are listed in Supplementary Table S2. All cell lines were cultured in a humidified atmosphere with 5% CO_2 at 37 °C in RPMI 1640 medium (Sigma-Aldrich) with 10% fetal bovine serum (FBS) (Life Technologies) and 2 mM L-glutamine (Merck KGaA), with some exceptions based on specific cell requirements. The OAW42 cell lines were maintained in Minimum Essential Medium Eagle (EMEM, Sigma-Aldrich). For CaOv3, Dulbecco's Modified Eagle's Medium (DMEMSigma-Aldrich, St.), was used. Finally, the OV90 cell line was cultured in Dulbecco's Modified Eagle's Medium and Ham's F12 (DMEM/F-12Sigma-Aldrich), to better match their growth requirements.

A431tFR and A431tMock cells were obtained in-house by transfection[36].

Primary ovarian cancer cell line (POCC) cultures (POCC1, POCC3, and POCC4), were established in-house from the ascitic fluid obtained from three patients undergoing debulking surgery for a confirmed diagnosis of ovarian cancers. Ascitic fluid samples, collected during routine medical procedures, were made available for research purposes, in accordance with the institutional guidelines. Clinical details were recorded, and samples were assigned with a reference number to retain anonymity.

FreeStyle™ 293 (Invitrogen) were cultured in Gibco® FreeStyle™ 293 Expression Medium (Invitrogen) in shaker flasks. The flasks were placed on an orbital shaker platform at 125 rpm, in a humidified atmosphere containing 8% CO_2 at 37 °C.

Plasmid generation, transfection, antibody production and purification

The variable VH and VL sequences of AFRA5.3 were cloned into pVITRO hIgG1K plasmid using the Polymerase Incomplete Primer Extension (PIPE) cloning method[37] to generate the fully human AFRA hIgG1. A schematic representation of the AFRA hIgG1 cassette inserted in the vector is shown in Supplementary Figure S1.

The AFRA hIgG1 pVITRO vector was transfected into FreeStyle™ 293 cells following the manufacturer's instruction for FreeStyle™ Max Reagent (Invitrogen). After 15 days of selection with Higromycin B Gold (InvivoGen), the cells expressing AFRA hIgG1 were expanded until days 13–15 to maximize expression yield. Purification of AFRA hIgG1 from cell culture supernatant was performed on HiTrap® Protein A column connected to an AKTA GO chromatography system (Cytiva,). The column was equilibrated with 20 mM sodium phosphate buffer (pH 7.4), followed by sample loading and washing with the same buffer. The antibody was eluted with 0.1 M glycine-HCl (pH 2.8) and the most concentrated eluted fractions were collected.

The size, homogeneity, and potential aggregation were analysed by sodium dodecyl sulphate–polyacrylamide gel electrophoresis (SDS–PAGE) and Size Exclusion Chromatography (SEC).

SEC was carried out on a Superdex 200 5/15 column (Cytiva) connected to a High Performance Liquid Chromatography (HPLC Series 200, Perkin Elmer), as described in[38]. Briefly, the mobile phase consisted of 10

mM sodium phosphate buffer pH 7.4 with 150 mM sodium chloride, delivered at a flow rate of 0.3 mL/min for a total run time of 10 min. The volume of each sample loaded onto the column was 10 µl.

The theoretical isoelectric point (pI) of each peptide was calculated by the Expasy ProtParam online tool.

ELISA assay

IGROV1, A431tFR, A431, and A431tMock cells were seeded at 4×10^4 cells/well and cultured as monolayers in 96-well flat bottom plates (Corning Incorporated). Cells were fixed with 0.1% glutaraldehyde (Sigma-Aldrich) and blocked with PBS + BSA 1% (Sigma-Aldrich). AFRA hIgG1 and ChiMOv19 were tested in serial dilution ranging from 2.5 µg/mL to 0.0025 µg/mL. Binding was detected using Anti-human IgG-HRP (Sigma-Aldrich St.) diluted 1:1000 in PBS + BSA 0.03%. All the assays were developed using 3',3',5',5'TetraMethylBenzidine (TMB Sigma-Aldrich) and stopped after 10 min with 1 M H_2SO_4 (Merck KGaA)[39]. Optical densities were measured at 450 nm using a spectrophotometer (IMark Microlplate Reader, Bio-Rad).

Flow cytometry assay

Binding of AFRA hIgG1 and ChiMOv19 was assessed by flow cytometry on a large panel of cancer cell lines and primary cultures known to express FRα and, as specificity control, on a tumor cell line with ectopic expression of FRα (A431tFR) and the corresponding isogenic negative controls (A431 and A431tMock). Briefly, AFRA hIgG1 and ChiMOv19 were used at high concentrations (10 µg/mL), to achieve the antigen saturation and detected with an Alexa-488 anti-human IgG (H + L) diluted 1:500 (Invitrogen).

The AFRA hIgG1 competitive binding assay was performed on IGROV1, an ovarian cancer cell line highly expressing FRα. Tumor cells were simultaneously incubated at 4 °C for 30 min with a fixed concentration of 10 µg/mL of Alexa-488 conjugated AFRA hIgG1 antibody and unlabeled ChiMOv19 and ChiMOv18 antibodies tested in serial dilutions ranging from 100 µg/mL to 0.1 µg/mL, using a 1:10 dilution factor. Alexa-488 labeling of AFRA hIgG1 antibody was performed using Alexa Fluor 488 Protein labeling Kit (Life Technologies). After incubation, cells were washed, and the Alexa-488 mean fluorescence intensity (MFI) was evaluated by flow cytometry using a FACS CANTO (Becton Dickinson) and data analyzed using Flow JO software (Becton Dickinson,).

Surface plasmon resonance (SPR) analysis

SPR analyses were conducted using a Biacore T200 platform (Cytiva). The ligand was immobilized on a CM5 sensor chip (Cytiva) via standard EDC (N-ethyl-N-(3-dimethylaminopropyl) carbodiimide)/NHS (N-hydroxysuccinimide) coupling employing the Amino Coupling Kit (Cytiva) and following the manufacturer's protocol. One flow cell served as a reference, undergoing the same activation and blocking steps without protein immobilizzation. After activation of the chip surface with EDC/NHS, excess carboxyl groups were blocked with 1 M ethanolamine (pH 8.0). The analysis were performed at 25 °C and in HBS-EP + buffer. The flow rate for all assays was set at 30 µL/min, and the sensor surface was regenerated with 0.1 M glycine-HCl (pH 2.8) after each injection.

For intrinsic affinity measurements we used the multi-cycle kinetics (MCK) method; the antibodies (AFRA hIgG1 and ChiMOv19) were immobilized at 300–500 RU, and FRα produced in a baculovirus expression system (custom-made by AXXAM, Milan, Italy) was injected at serial dilutions ranging from 200 to 0.4 nM.

For functional affinity we used the single-cycle kinetics (SCK) method; recombinant FRα,, was immobilized at 700 RU. The antibody was injected in serial dilutions ranging from 12.5 to 0.8 nM without regeneration after each concentration.

For competitive binding, FRα was first immobilized at 500 RU, and each antibody was injected at 500 nM for three minutes.

To analyse binding responses, Biacore T200 Evaluation Software (Cytiva) was used, reporting results as response units (RU) over time.

Isolation and culture of effector cells

Healthy donor buffy coats were provided by the Immuno-Haematology and Transfusion Medicine Unit of our Institute after signing an informed consent form. The study, identified by the protocol number INT 56/19, was conducted in accordance with institutional guidelines and followed the principles of the Declaration of Helsinki. Peripheral blood mononuclear cells (PBMCs) were isolated from peripheral blood of healthy donors using Ficoll density gradient centrifugation (30 min at 500×g) using Ficoll-Paque™ PLUS (Cytiva). The PBMCs were frozen in FBS with 10% dimethyl sulfoxide (Sigma-Aldrich) in liquid nitrogen. A total of 20×10^6 cells per vial were frozen, with a viability of 90%. Before each experiment, PBMCs were thawed and resuspended in prewarmed TexMACS™ culture medium (Miltenyi Biotech) for 24 h (no interleukins were added). After thawing and culture we recovered about $14–16 \times 10^6$ cells/vial, with a relative viability around 80%.

Cytotoxicity assay

For the evaluation of cytotoxicity, a panel of tumor cell lines of different origin and primary tumor cultures were seeded on 96-well flat bottom plates (Corning Incorporated) and after 24 h of adhesion they were treated with antibodies alone (AFRA hIgG1 and ChiMOv19) at 2 µg/mL or with antibodies plus PBMCs (E: T, 10:1); at the end of the experiments tumour cells were washed twice with PBS and viable cells were detected using the CellTiter-Glo® Luminescent Cell Viability Assay (Promega). Tumor cells alone and tumor cells with PBMCs alone were used as controls. The percentage of inhibition was calculated using with the following formula: % specific lysis = (1 – chemiluminescence reading of treated cells/chemiluminescence reading of untreated cells) ×100.

Statistical analysis

Statistical analysis was performed using GraphPad Prism software (version 5.02). Non-parametric student's *t*-test was used to determine the significance of differences between treatments.

Data are not considered statistically significant unless indicated in the figures (* $p<0.05$; ** $p<0.01$; *** $p<0.001$ ns $p>0.1$).

Data availability

All data generated or analysed during this study are included in this published article and its supplementary information files. The Uncropped supplementary Figure S2 and uncropped supplementary Figure S3 have been addedThe original output of the Biacore data are available as row data but the biacore program is neded to open them (.bme); All the row data are available upon request by contacting the corresponding author (Mariangela. figini@istitutotumori.mi.it).

Received: 2 July 2025; Accepted: 12 December 2025
Published online: 31 December 2025

References

1. Nawaz, F. Z. & Kipreos, E. T. Emerging roles for folate receptor FOLR1 in signaling and cancer. *Trends Endocrinol. Metab.* **33** (3), 159–174 (2022).
2. Scaranti, M., Cojocaru, E., Banerjee, S. & Banerji, U. Exploiting the folate receptor α in oncology. *Nat. Rev. Clin. Oncol.* **17** (6), 349–359 (2020).
3. Cheung, A., Bax, H. J., Josephs, D. H., Tutt, A. N. & Karagiannis, S. N. Targeting folate receptor alpha for cancer treatment. *Oncotarget* **7** (32), 52553–52574 (2016).
4. Frigerio, B., Bizzoni, C., Jansen, G., Matherly, L. H. & Figini, M. Folate receptors and transporters: Biological role and diagnostic/therapeutic targets in cancer and other diseases. *J. Experimental Clin. Cancer Res.* **38** (1), 125 (2019).
5. Ornella, M. S. C. et al. Immunotherapy for peritoneal carcinomatosis: Challenges and prospective outcomes. *Cancers* **15** (8), 2383 (2023).
6. Baydoun, M. et al. Folate receptor targeted photodynamic therapy: A novel way to stimulate Anti-Tumor immune response in intraperitoneal ovarian cancer. *Int. J. Mol. Sci.* **24** (14), 11288 (2023).
7. Qi, J., Hymel, D., G Nelson, C., R Burke, T. & Rader, C. Conventional and chemically programmed asymmetric bispecific antibodies targeting folate receptor 1. *Front. Immunol.* **10**, 1994 (2019).
8. Young, O. et al. Folate receptor as a biomarker and therapeutic target in solid tumors. *Curr. Probl. Cancer*. **47** (1), 100917 (2023).
9. Tamura, N. et al. Correlation between the expression of folate receptor alpha (FRα) and clinicopathological features in patients with lung adenocarcinoma. *Lung Cancer*. **145**, 152–157 (2020).
10. Kumari, L. et al. Emerging targeted therapeutic strategies for the treatment of triple-negative breast cancer. *J. Drug Target.* **31** (9), 889–907 (2023).
11. Schnoell, J. et al. Protein expression of folate receptor alpha in adenoid cystic carcinoma of the head and neck. *Onco Targets Ther.* **15**, 531–538 (2022).
12. Despierre, E. et al. Folate receptor alpha (FRA) expression remains unchanged in epithelial ovarian and endometrial cancer after chemotherapy. *Gynecol. Oncol.* **130** (1), 192–199 (2013).
13. Crane, L. M. A. et al. The effect of chemotherapy on expression of folate receptor-alpha in ovarian cancer. *Cell. Oncol. (Dordr)*. **35** (1), 9–18 (2012).
14. Miotti, S. et al. Characterization of human ovarian carcinoma-associated antigens defined by novel monoclonal antibodies with tumor-restricted specificity. *Int. J. Cancer*. **39** (3), 297–303 (1987).
15. Frigerio, B., Montermini, M., Canevari, S. & Figini, M. Role of antibody engineering in generation of derivatives starting from MOv19 mab: 40 years of biological/therapeutic tools against folate receptor Alfa. *Antib. Ther.* **5** (4), 301–310 (2022).
16. Matulonis, U. A. et al. Efficacy and safety of Mirvetuximab Soravtansine in patients with Platinum-Resistant ovarian cancer with high folate receptor alpha expression: results from the SORAYA study. *J. Clin. Oncol.* **41** (13), 2436–2445 (2023).
17. Moore, K. N. et al. Mirvetuximab Soravtansine in FRα-Positive, Platinum-Resistant ovarian cancer. *N Engl. J. Med.* **389** (23), 2162–2174 (2023).
18. Dilawari, A. et al. FDA approval summary: Mirvetuximab Soravtansine-Gynx for FRα-Positive, Platinum-Resistant ovarian cancer. *Clin. Cancer Res.* **29** (19), 3835–3840 (2023).
19. Shah, P. et al. 431 First-in-human phase I clinical trial evaluating intraperitoneal administration of MOv19-BBz CAR T cells in patients with alpha folate receptor-expressing recurrent high grade serous ovarian cancer. *J. Immunother. Cancer* **9**(Suppl 3): A461–A461. https://jitc.bmj.com/content/9/Suppl_2/A461 (2021).
20. Jespers, L. S., Roberts, A., Mahler, S. M., Winter, G. & Hoogenboom, H. R. Guiding the selection of human antibodies from phage display repertoires to a single epitope of an antigen. *Biotechnol. (N Y)*. **9**, 899–903 (1994).
21. Figini, M. et al. Panning phage antibody libraries on cells: isolation of human fab fragments against ovarian carcinoma using guided selection. *Cancer Res.* **58** (5), 991–996 (1998).
22. Figini, M. et al. Conversion of murine antibodies to human antibodies and their optimization for ovarian cancer therapy targeted to the folate receptor. *Cancer Immunol. Immunother*. **58** (4), 531–546 (2009).
23. Zacchetti, A. et al. Antitumor effects of a human dimeric antibody fragment 131I-AFRA-DFM5.3 in a mouse model for ovarian cancer. *J. Nucl. Med.* **52** (12), 1938–1946 (2011).
24. Coney, L. et al. Chimeric murine-human antibodies directed against folate binding receptor are efficient mediators of ovarian carcinoma cell killing. *Cancer Res.* **54**, 2448–2455 (1994).
25. Casalini, P. et al. Unidirectional potentiation of binding between two anti-FBP mabs: evaluation of the involved mechanisms. *J. Cell. Biochem.* **58** (1), 47–55 (1995).
26. Satta, A. et al. A bispecific antibody to link a TRAIL-Based antitumor approach to immunotherapy. *Front. Immunol.* **10**, 2514 (2019).
27. Bax, H. J. et al. Folate receptor alpha in ovarian cancer tissue and patient serum is associated with disease burden and treatment outcomes. *Br. J. Cancer*. **128** (2), 342–353 (2023).
28. Ebel, W. et al. Preclinical evaluation of MORAb-003, a humanized monoclonal antibody antagonizing folate receptor-alpha. *Cancer Immun.* **7**, 6 (2007).
29. Mazor, Y. et al. Enhancement of immune effector functions by modulating IgG's intrinsic affinity for target antigen. *PLoS ONE*, **11** (6), 1–20 (2016).
30. Wang, R. et al. Antibody-Drug conjugates (ADCs): current and future biopharmaceuticals. *J. Hematol. Oncol.* **18** (1), 51 (2025).
31. Evans, R. et al. Design of high avidity and low affinity antibodies for in situ control of antibody drug conjugate targeting. *Sci. Rep.* **12** (1), 7677 (2022).

32. Rudnick, S. I. et al. Influence of affinity and antigen internalization on the uptake and penetration of Anti-HER2 antibodies in solid tumors. *Cancer Res.* **71** (6), 2250–2259 (2011).
33. Fujimori, K., Covell, D. G., Fletcher, J. E. & Weinstein, J. N. A modeling analysis of monoclonal antibody percolation through tumors: A binding-site barrier. *J. Nucl. Med.* **31** (7), 1191–1198 (1990).
34. van Osdol, W., Fujimori, K. & Weinstein, J. N. An analysis of monoclonal antibody distribution in microscopic tumor nodules: Consequences of a 'binding site barrier'. *Cancer Res.* **51** (18), 4776–4784 (1991).
35. Bordeau, B. M., Yang, Y. & Balthasar, J. P. Transient competitive Inhibition bypasses the binding site barrier to improve tumor penetration of trastuzumab and enhance T-DM1 efficacy. *Cancer Res.* **81** (15), 4145–4154 (2021).
36. Coliva, A. et al. 90Y labeling of monoclonal antibody MOv18 and preclinical validation for radioimmunotherapy of human ovarian carcinomas. *Cancer Immunol. Immunother.* **54** (12), 1200–1213 (2005).
37. Dodev, T. S. et al. A tool kit for rapid cloning and expression of Recombinant antibodies. *Sci. Rep.* **4**, 5885 (2014).
38. Frigerio, B. et al. A single-chain fragment against prostate specific membrane antigen as a tool to build theranostic reagents for prostate cancer. *Eur. J. Cancer.* **49** (9), 2223–2232 (2013).
39. Tabatabaei, M. S. & Ahmed, M. Enzyme-Linked immunosorbent assay (ELISA). *Methods Mol. Biol.* **2508**, 115–134 (2022).

Acknowledgements
We thank Dr. Flavio Arienti and the Immuno-Hematology and Transfusion Medicine Unit who supplied buffy coats and blood samples for PBL extraction.

Author contributions
Mariangela Figini: conception and design of the study. Elena Luison, Davide Tresoldi, Valeria Arlotta, Elena Pinto: *in vitro* functional and biological characterization of AFRA hIgG1. Elena Luison, Valeria Arlotta, Elena Pinto: production and purification of the IgG and technical support *in vitro* experiments. Mariangela Figini, Delia Mezzanzanica, Silvana Canevari, Barbara Frigerio, Elena Luison, Valeria Arlotta, Elisa Corsiero, Francesco Raspagliesi: acquisition, analysis of data, interpretation of data and drafting the manuscript. Mezzanzanica Delia, Sophia Karagiannis, Silvana Canevari, Mariangela Figini: final revision of the manuscript and enhancement of its intellectual content. All authors reviewed the results and approved the final version of the manuscript.

Funding
This work was supported by the European Union—Next Generation EU—NRRP M6C2—Investment 2.1 Enhancement and strengthening of biomedical research in the NHS (project #PNC-E3-2022-23683269-PNC-HLS-TA).

Declarations

Competing interests
The authors declare no competing interests.

Ethics approval
I confirm that the use of the patients ascitic fluid cells has been approved by the ethical committee CET Lombardia 4; identificative number INT131/23.

Consent to participate
Ascitic fluid samples, collected during routine medical procedures, were made available for research purposes, in accordance with the institutional guidelines. Clinical details were recorded, and samples were assigned with a reference number to retain anonymity.

Additional information
Supplementary Information The online version contains supplementary material available at https://doi.org/10.1038/s41598-025-32752-x.

Correspondence and requests for materials should be addressed to M.F.